

# Modeling and simulating an aftershock process caused by a strong earthquake in the Barents Sea shelf

Sergey Baranov<sup>1</sup>

Received 20 April 2011; accepted 26 April 2011; published 4 May 2011.

The paper considers an aftershock process caused by an  $M_w = 6.1$  earthquake which occurred on 21 February 2008 in the Storfjord channel (Spitsbergen). The earthquake was the strongest in the history of seismic monitoring on the Barents Sea shelf. To study the aftershock process, some relaxation models of aftershock decay rate and the Epidemic-type Aftershock-sequences (ETAS) model of triggered seismicity were fitted. It was shown that the aftershock process was a superposition of two subprocesses relaxation and trigger. Each of the subprocesses was simulated using a relevant model. Based on the modeling, a hypothesis of Storfjord seismicity connected with fluid effect on the local stress field was suggested. *GCMD TERMS:* Solid Earth; Seismology; Earthquake Dynamics / Earthquake Occurrence; *KEYWORDS:* Aftershock process; model of aftershock decay rate; ETAS model; aftershock process simulating; Spitsbergen.

**Citation:** Baranov, Sergey (2011), Modeling and simulating an aftershock process caused by a strong earthquake in the Barents Sea shelf, *Russ. J. Earth. Sci.*, 12, ES1002, doi:10.2205/2011ES000502.

## Introduction

Spitsbergen (Svalbard) Archipelago is located on a passive continental margin of the Eurasian plate which is abutted at zones of ultra slow spreading in the North Atlantic (Svalbard fault zone (SFZ), Mon and Knipovich Ridges) and Arctic Oceans (Gakkel Ridge). The spreading rates vary from 0.15 to 0.5 cm per year in Knipovich Ridge, 1.3 – 2.0 cm per year in Mon Ridge [Crane *et al.*, 1982], and approximately 0.9 – 1.1 cm per year in Gakkel Ridge [Michael *et al.*, 2003]. The majority of strong earthquakes have occurred in a narrow area extending along the Mon and Knipovich Ridges (Figure 1a). The central areas of the Barents–Kara plate are almost aseismic, except the West margin of the Barents Sea shelf, including the continental slope and Svalbard elevation. The most active zone not only in the Svalbard elevation but also in the entire European Arctic is the Storfjord channel (Figure 1b) which seismicity can hardly be explained by the known faults, both in the sea bottom and land.

The Storfjord channel delimits two of the largest Svalbard islands – Edge and West Spitsbergen. The first instrumentally recorded surge of seismic activity was in 1976, when on

18 January at 0446:26 UT a  $m_b = 5.5$  earthquake occurred in Heer Land (West coast of Storfjord; Figure 1b). The hypocenter depth estimations vary from 10 (CSEM, Centre Sismologique Euro-Mediterraneen) to 46.8 km (ISC, International Seismological Centre). The earthquake was followed by a large number of aftershocks [Bungum *et al.*, 1982]. In 1977–1984, more than 2000 aftershocks with magnitudes less than 3.5 were registered in a rectangle of  $40 \times 50$  km centered in the epicenter [Panasenko *et al.*, 1987]. After January 1976 there were no strong earthquakes in Storfjord till 2003, when on 4 June at 0716:43 UT an  $M_w = 5.1$  earthquake occurred in Zuydcapp (Figure 1). The hypocenter depth estimations vary from 10 (NEIC, National Earthquake Information Center) to 44 km (NAO, NORSAR, Norwegian Seismic Array). Unlike the earthquake in 1976 this event did not generate numerous aftershocks (5 events with  $ML > 2$ ).

After the earthquake in 2003, no appreciable events were observed in the area during 6 years. The situation changed in 2008 when on 21 February at 0246:17.41 UT the strongest  $M_w = 6.1$  earthquake occurred in the Storfjord channel. Macroseismic effect produced by the earthquake was described in [Baranov *et al.*, 2008]. The mainshock generated a lot of aftershocks. In the first days the intensity of the aftershock process reached more than 950 events per day. During 2008 more than 3000  $ML > 1$  aftershocks were recorded. Until now the seismic activity has not returned to the background level. The paper considers the aftershock process of the  $M_w = 6.1$  earthquake in Storfjord using the relaxation models of the aftershock decay rate and the Epidemic-type Aftershock-sequences (ETAS) model of triggered seismicity.

<sup>1</sup>Kola Branch of Geophysical Survey of RAS, Apatity, Murmansk Region, Russia

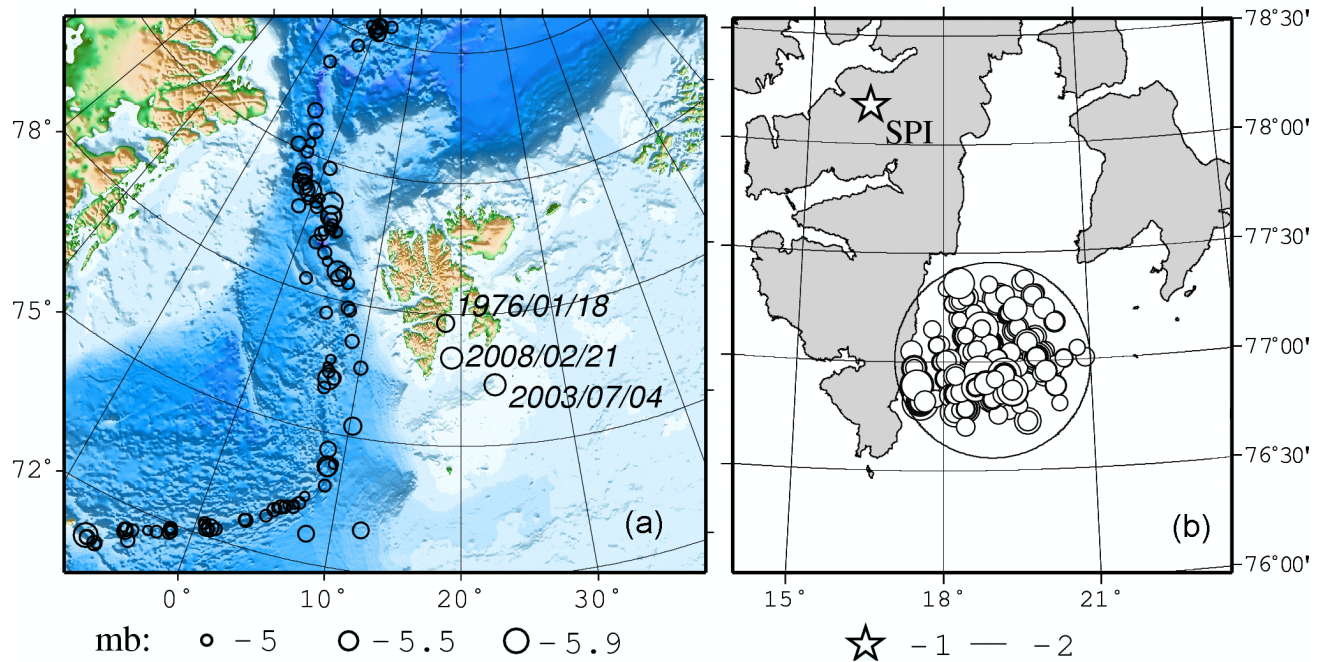


**Figure 1.** (a) –  $mb > 5$  earthquakes which occurred in Spitsbergen in 1976–2009; (b) –  $ML > 2$  aftershocks of the  $M_w = 6.1$  earthquake on 21 February 2008 for the period of 21 February 2008–10 April 2009. (1 – seismic group SPI; 2 – aftershock area.)

## Localization of Aftershock Area and Data Used

To study the aftershock process, we used data recorded by the Norwegian seismic array SPI consisting of 9 one-type broadband seismometers. The aperture (distance between the sensors) is 1 km. The SPI group is situated at the point of 78.178 N and 16.37 E near Longyearbyen at a distance of 150 km North of the aftershock area (Figure 1b).

The most accurate estimation of the mainshock epicenter made using the data of 10 regional network stations is 77.007 N and 19.008 E, the depth varying from 15 to 20 km [Pirly *et al.*, 2010]. The moment tensor of the mainshock describes oblique-normal faulting according to the regional and teleseismic waveform modeling.

For localizing the aftershock area, Pirly *et al.* [2010] calculated the coordinates of 256 aftershocks with magnitudes greater than 1.7 by means of an original method of body wave inversion. The area is bounded by a circle with a radius 50 km centered at the mainshock epicenter (Figure 1b).

During the first days after the mainshock the intensity of the aftershock process exceeded 950 events per day. To automate the processing of such a big data volume a special program UDL was developed [Asming and Fedorov, 2010]. The program detects and locates events occurring in Storfjord using the data recorded by SPI seismic group. The list of events obtained by UDL contains information on earthquakes with magnitudes  $ML$  from  $-1.2$  to 6 (the mainshock) for the period of 1 January 2008–10 April 2010 (Figure 2a). The completeness magnitude is  $-0.2$  (Figure 2b). So we

will consider the events with  $ML \geq 2$  only. The final catalog contains information on 29,403 events.

## Tested Models and Fitting Method

The traditional approach to studying seismicity surges involves treating them as a point process which is completely described by conditional intensity [Liptzer and Shiriyev, 2000]:

$$n(t|H_t) = \lim_{h \rightarrow 0} P([t, t+h]) / h \quad (1)$$

where  $P([t, t+h])$  is a probability that an event (aftershock) occurs in the time interval  $[t, t+h]$ ;  $H_t$  is the history of event times preceding  $t$ . Let us denote  $n(t) = n(t|H_t)$  for simplicity. From the seismological point of view  $n(t)$  is just number of earthquakes per unit time. So, different models of aftershock processes have different functions  $n(t)$ .

To study the aftershock processed in Storfjord we used relaxation (hyperbolic and exponential) models of the aftershock decay rate and the ETAS model of trigger seismicity. In relaxation models the number of aftershocks per unit time is controlled by stress relaxation in the fault zone. Therefore these models take into account the aftershocks occurrence times ignoring their magnitudes. In experiments on fracture mechanics microfracturing of the hyperbolic type is observed if one relieves loading just after the fracturing process has begun. The exponential type of microfracturing emerges when

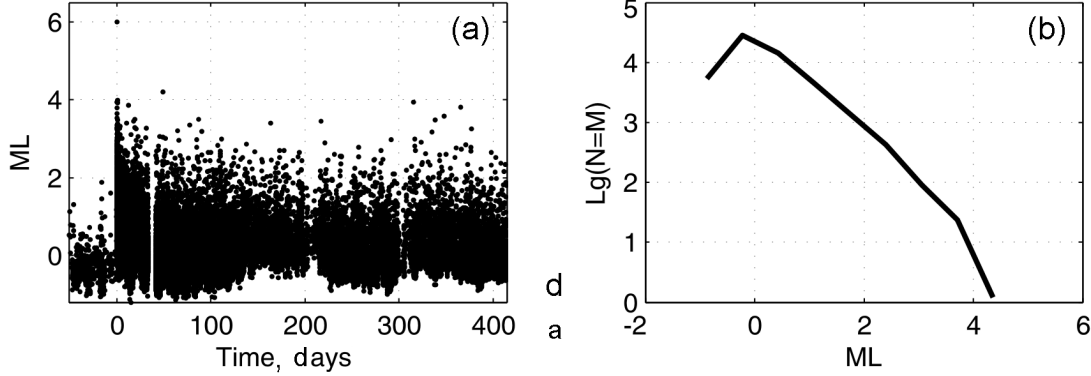


**Figure 2.** Seismicity of the Storfjord channel for the period of 1 January 2008–10 April 2009 – result of UDL program. (a) The earthquake magnitudes as a function of their occurrence (0 at the horizontal axis corresponds to 21 February 2008, 0246:17.41 UT – the mainshock time). (b) A magnitude-frequency relation for the earthquakes.

loading is not relieved during the fracturing. In practice identifying the type of aftershock process is difficult because the type can change from hyperbolic to exponential not long after the mainshock time [Narteau *et al.*, 2002; Sholz, 1968].

As a hyperbolic relaxation model a modified Omori law (MOL) [Utsu, 1961] was applied:

$$n(t) = K/(t + c)^p \quad (2)$$

where  $n(t)$  – the number of aftershocks per unit time;  $K$ ,  $c$ ,  $p$  are the model parameters.

The general model of exponential type, called a modified stretched exponent (MSTREXP) and suggested by Kisslinger [1993], is defined by

$$n(t) = qN^* \exp\left[\left(\frac{d}{t_0}\right)^q\right] \frac{1}{t+d} \times \left(\frac{t+d}{t_0}\right)^q \exp\left[-\left(\frac{t+d}{t_0}\right)^q\right] \quad (3)$$

where  $d$ ,  $t_0$  (relaxation time),  $q \leq 1$ , and  $N^*$  are the fitted parameters. It was shown that MSTREXP describes some aftershocks sequences in California better than MOL [Gross and Kisslinger, 1994].

The models (2) and (3) were obtained experimentally. The limited power law (LPL) model was deduced analytically [Narteau *et al.*, 2002]. It describes both hyperbolic and exponential types of aftershock sequences and transition from one to the other as well. The LPL model is defined by

$$n(t) = A \times t^{-q} [\gamma(q, \lambda_b t) - \gamma(q, \lambda_a t)] \quad (4)$$

where  $\gamma(\rho, x)$  is an incomplete gamma function;  $A$ ,  $q$ ,  $\lambda_a$ , and  $\lambda_b$  are the fitted parameters.

The models (2)–(4) were also used with background seismicity,  $r$  (events per day), i.e.  $n(t) = n(t) + r$ .

In the models (2)–(4) the number of aftershocks per unit time depends on their occurrence times and the magnitudes

being ignored. To take into account the magnitudes we have tested the ETAS model of triggered seismicity suggested by Ogata [1999]:

$$n(t) = \mu + \sum_{t_i \leq t} \frac{K_i}{(t - t_i + c)^p}$$

$$K_i = K_0 \exp[\alpha(M_i - M_0)] \quad (5)$$

where  $t_i$  – time and  $M_i$  – magnitude of the event with number  $i$  from the catalog;  $M_0$  – cut-off magnitude;  $\mu$  (background seismicity),  $K_0$ ,  $c$ , and  $p$  are the fitted parameters.

Summation in (5) is executed for all aftershocks occurring before time  $t$ . The number of aftershocks in time  $t$  depends on background seismicity and observations in previous times which are represented by superposition of Omori law sequences. So  $K_i$  in (5) represents an impact of aftershock with magnitude  $M_i$  occurring in time  $t_i$  to the triggered sequence. Since the ETAS model takes into account full information on the process, it gives a better approximation of cumulative curve  $N(t)$  which is an integral of  $n(t)$ .

All the models were fitted with the maximum likelihood method. The log likelihood function is defined by [Daley and Vere-Jones, 1972; Ogata *et al.*, 1993]:

$$\ln L(\theta) = \sum_{i=1}^N \ln n(t_i) - \int_{T_0}^{T_1} n(t) dt, \quad (6)$$

where  $N$  – number of aftershocks;  $T_0$ ,  $T_1$  – observation time;  $n(t)$  is the conditional intensity (2)–(5) of the aftershock process. To estimate the model parameters one should maximize (6) with respect to  $\theta$ .

To choose the best models we used Akaike information criterion (AIC) and Bayesian information criterion (BIC) in the form suggested in [Leonard and Hsu, 1999]:

$$\text{AIC} = -2 \max_{\theta} \{\ln L(n(\theta))\} + 2k \quad (7)$$

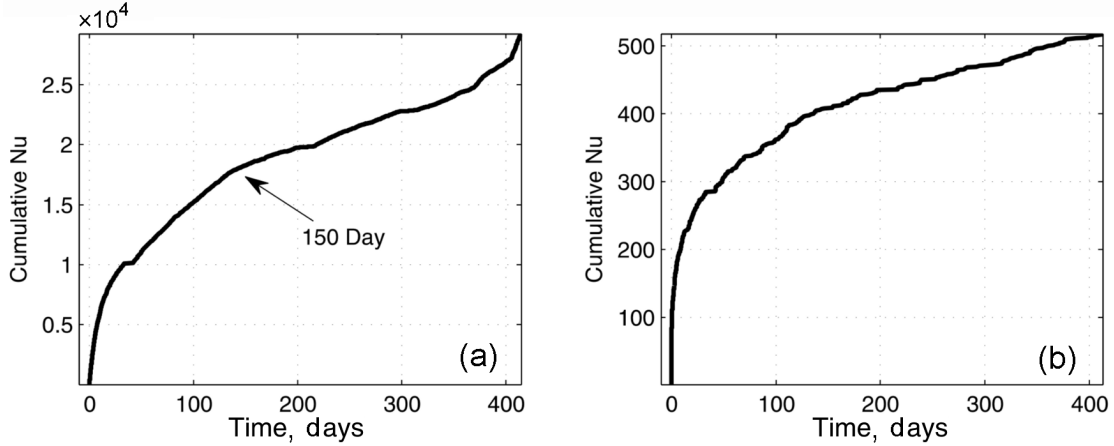


**Figure 3.** Cumulative number for aftershocks with  $ML \geq -0.2$  (a) and  $ML \geq 2$  (b).

$$BIC = -\max_{\theta} \{\ln(L(n\theta))\} + \frac{k}{2} \ln \frac{N}{2\pi} \quad (8)$$

where  $k$  is the number of fitted parameters,  $N$  – the number of events in catalog,  $\theta$  is a vector of model parameters,  $L$  is the likelihood function,  $n$  represents the model (2)–(5). The better the model, the lower AIC and BIC values it has.

## Results of Storfjord Aftershock Process Modeling

The cumulative number of  $ML \geq -0.2$  aftershocks changes its convexity after about 150 days (Figure 3a). This

peculiarity disappears if one increases the low magnitude limit up to 2 (Figure 3b). It means that the aftershocks with  $ML \geq -0.2$  cannot be described by a relaxation model as the second derivative  $N''(t) = n'(t)$  is always negative, i.e., the number of aftershocks per unit time is a decreasing function. The cumulative curve for a  $ML \geq 2$  aftershock sequence has a regular form that can be approximated by relaxation models. Thus the sequences of aftershocks with  $ML \geq -0.2$  and  $ML \geq 2$  should be considered separately.

The results of estimating the models parameters and the values of AIC and BIC are shown in Table 1. For  $ML \geq -0.2$  the parameter estimations poorly agree with values obtained for other regions (see [Gross and Kisslinger 1994; Narreau et al., 2002]). We explain this by the fact that the cumulative curve changes its convexity (Figure 3a). It should be

**Table 1.** Estimated parameters of the models (2)–(5) and the values of AIC and BIC

| Model                               | Parameters  | AIC        | BIC        |
|-------------------------------------|---|------------|------------|
| $ML \geq -0.2$ (29,246 Aftershocks) |   |            |            |
| Omori (2)                           | $K = 1047.68; c = 0.47; p = 0.58$   | -209,955.5 | -104,968.1 |
| Omori + Background (2)+ $r$         | $K = 78,069.07; c = 9.85; p = 1.88; r = 43.12$                            | -211,940.5 | -105,957.4 |
| MSTREXP (3)                         | $q = 0.42; N^* = 5,235,519.9; d = 0.459; t_0 = 140$                       | -209,962.1 | -104,968   |
| MSTREXP + Background (3) + $r$      | $q = 0.31; N^* = 11,195.4; d = 5.7; t_0 = 0.85; r = 43.71$                | -211,959.2 | -105,963.5 |
| LPL (4)                             | $A = 850.83; \lambda_a = 0.001; \lambda_b = 2.136; q = 0.39$              | -207,865   | -103,919.6 |
| LPL + Background (4) + $r$          | $A = 20,650; \lambda_a = 0.024; \lambda_b = 752.96; q = 0.013; r = 44.83$ | -211,702.4 | -105,835.1 |
| ETAS (5)                            | $\mu = 1.58; K = 0.103; c = 0.138; \alpha = 0.26; p = 2.11$               | -221,204.8 | -110,586.3 |
| $ML \geq 2$ (518 Aftershocks)       |   |            |            |
| Omori (2)                           | $K = 34.49; c = 0.006; p = 0.797$   | -642.6     | -317.7     |
| Omori + Background (2)+ $r$         | $K = 3.48; c = 0.009; p = 0.839; r = 0.127$                               | -643.6     | -318.2     |
| MSTREXP (3)                         | $q = 0.21; N^* = 14,868.3; d = 0.002; t_0 = 300$                          | -649.2     | -319.8     |
| MSTREXP + Background (3) + $r$      | $q = 0.18; N^* = 8253.69; d = 0.004; t_0 = 400; r = 0.12$                 | -649.6     | -318.8     |
| LPL (4)                             | $A = 34.66; \lambda_a = 0.001; \lambda_b = 284.4; q = 0.75$               | -636.9     | -313.6     |
| LPL + Background (4) + $r$          | $A = 33.25; \lambda_a = 0.001; \lambda_b = 147.038; q = 0.82; r = 0.21$   | -650.6     | -319.2     |
| ETAS (5)                            | $\mu = 0.07; K = 0.01; c = 0.004; \alpha = 1.91; p = 0.91$                | -679.8     | -333.9     |

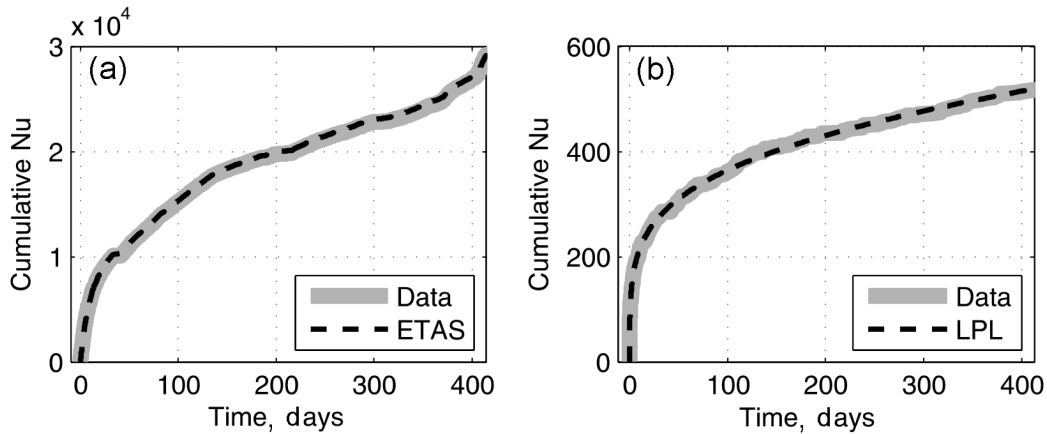


**Figure 4.** Cumulative number aftershocks as a function of time observed in Storfjord compared with those expected by the ETAS model (a) and LPL model (b).

noted that modeling of aftershock processes with such an irregularity as in Storfjord was not referred to in these works. The best model for  $ML \geq -0.2$  is ETAS (5). The estimated value of background seismicity,  $\mu$ , equals 1.6 events per day, it matches to seismic monitoring data and leads to 664 events per day. This means that 2.3% of all aftershocks during 415 days were externally triggered. Most of them represented a self triggered activity. Comparing the observed number of aftershocks and that expected by the ETAS model as a function of time (Figure 4a) one can see that the shape of both curves is almost identical.

One can conclude that the  $ML \geq -0.2$  aftershock process belongs to the trigger type as its cumulative curve has an irregular shape (Figure 3a) and the values of AIC and BIC for the relaxation models are greater than those for the ETAS model. This means that the aftershock number is not controlled just by the stress relaxation in the fault zone.

For the  $ML \geq 2$  aftershock sequence the parameters estimations (Table 1) agree with those obtained for other regions [Gross and Kisslinger 1994; Narreau *et al.*, 2002]. In this case ETAS model (5) also gives the best approximation of the cumulative curve. The estimated value of background seismicity,  $\mu$ , equals 0.07 events per day and matches to seismic monitoring data. The regular shape of the cumulative curve (Figure 3b) and small differences between AIC and BIC values for the relaxation and ETAS models allow to describe the sequence by relaxation laws of the aftershock decay rate.

According to AIC, the best choice among the relaxation models is an analytically deduced LPL model (4) with background seismicity (Table 1). The observed and the expected by LPL model numbers of aftershocks are almost the same (Figure 4b). This model describes both hyperbolic and relaxation aftershock processes, therefore one has to test other models to find out which type the aftershock process belongs to. According to BIC the best relaxation model is MSTREXP with no background. MOL and MSTREXP have similar AIC and BIC values. This peculiarity mentioned by many researchers makes identifying the type of an aftershock process difficult [Narreau *et al.*, 2002; Sholz,

1968]. Since the MSTREXP model (3) has lower values of AIC and BIC, we refer the  $ML \geq 2$  sequence to the exponential type. According to the laboratory experiments [Benioff, 1962; Sholz, 1968] it means that forces which caused the mainshock are still affecting the fault zone volume and more aftershocks with  $ML \geq 2$  will occur in the area.

In this section it has been shown that the aftershock process in Storfjord is a superposition of two subprocesses one of each (aftershocks with  $ML \geq 2$ ) has a relaxation mechanism and the other (aftershocks with  $ML \geq -0.2$ ) has trigger one. In the trigger process 2.3% of all aftershocks were externally triggered. The majority is a self triggered activity.

## Simulation of the Aftershock Process in Storfjord

In order to check the ability of the ETAS model (5) to describe the interevent time of the aftershock process in Storfjord, Monte Carlo simulation of the ETAS model with the parameters from Table 1 was produced. The simulation was performed by a thinning method [Lewis and Shedler, 1979] which is based on approximating a nonstationary point process with piecewise constant rates Poisson processes. This approach allows to determine the aftershock rate at each time by the preceding events and the background rate according to (5). The magnitudes are taken from the catalog. An appropriate algorithm was described in [Ogata, 1999]. Simulation was stopped when the number of aftershocks reached that of the catalog. We simulated aftershock sequences with  $M \geq -0.2$  and  $ML \geq 2$  separately.

Observed and synthetic (simulated) aftershock sequences with  $ML \geq -0.2$  are shown in Figure 5. Similar to the observed aftershock sequence, the synthetic one consists of several subsequences (Figure 5a, b). There is some difference between the cumulative curves appearing after 100 days (Figure 5c). According to Kolmogorov-Smirnov test the, interevent times,  $\Delta t$ , for the observed and synthetic sequences have different distributions in spite of the fact that empir-

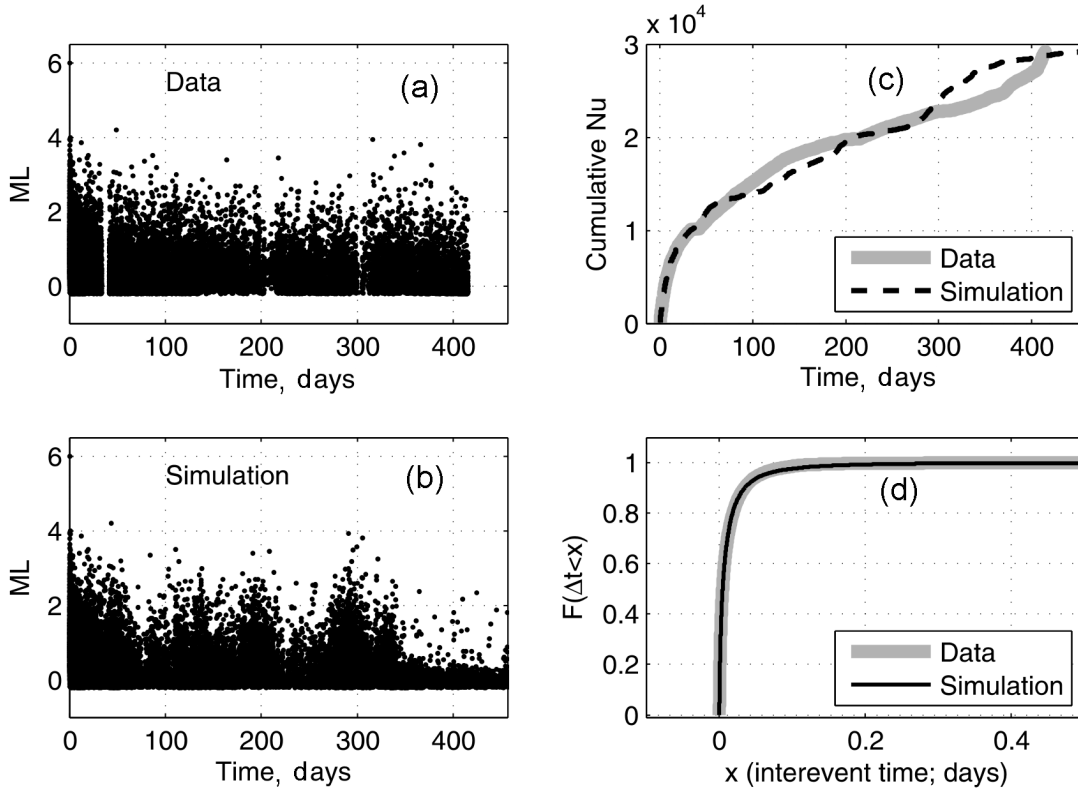


**Figure 5.** Simulation of the  $ML \geq -0.2$  aftershock process in Storfjord with ETAS model. (a) The observed and (b) synthetic aftershock sequences. (c) The observed and synthetic cumulative curves. (d) Empirical distribution functions of interevent times for the observed and synthetic aftershock sequences.

cal distribution curves seem to be identical (Figure 5d). The test statistics (absolute value of maximum of difference between the curves) equals 0.01, but the p-value (0.03) is less than 5% significance level.

To find out distributions of the observed and synthetic interevent times for  $M \geq -0.2$  aftershocks we fitted some distribution functions by means of the maximum likelihood method. The results are shown in Table 2. According to BIC criterion (8) the lognormal distribution gives a better fit than the others for the observed and synthetic aftershock sequences. Probability density of lognormal distribution is defined by

$$f(x|\mu, \sigma) = \exp\{-\ln x - \mu)^2 / 2\sigma^2\}, \quad x > 0$$

The parameters estimations (95% confidence interval) for the observed interevent times are  $\mu = -5.32 \pm 0.02$ ,  $\sigma = 1.49 \pm 0.01$  and for the synthetic ones  $\mu = -5.32 \pm 0.02$ ,  $\sigma = 1.55 \pm 0.01$ . The values of  $\mu$  are the same but  $\sigma$  are not. Thus, both the observed and synthetic interevent times have the only distribution with different parameters that confirms the result of Kolmogorov-Smirnov test. Verification by this way of 30 independent simulations has led to the same result. The quality of the distribution fit can be visualized by comparing the observed cumulative probabilities and those

calculated by means of lognormal distribution with  $\mu$  and  $\sigma$  shown above. The result is shown in Figure 6. The shape of the observed probability curve agrees with theoretical line, although there are some deflections for interevent of times less than 0.0007 and greater than 0.1 day. Though the part of such data amounts to less than 10%. Thus, the ETAS model with parameters from Table 1 adequately describes the form of distribution of interevent times for aftershocks with  $ML \geq -0.2$ .

The result of the ETAS model simulation of the aftershock process with  $ML \geq 2$  is shown in Figure 7. The observed and synthetic sequences are well consistent (Figure 7a, b). The cumulative curves of the aftershock number are almost identical (Figure 7c). According to Kolmogorov-Smirnov test, the interevent times of the observed and the synthetic sequences have the same distribution (Figure 7d): the test statistics is 0.04 and the p-value equals 0.996. Thus, the ETAS model describes well the time properties of the Storfjord aftershock processes with  $ML \geq 2$ .

To find out the distributions of the observed and synthetic interevent times for  $ML \geq 2$  aftershocks we, as in the case of  $ML \geq -0.2$  aftershocks, fitted some distribution functions by means of the maximum likelihood method. The results are shown in Table 2. Weibull distribution gives a better

**Table 2.** Maximal values of log likelihood functions (MaxLL) and BIC criterion (8) for estimating parameters of observed and synthetic interevent times for  $M \geq -0.2$  and  $ML \geq 2$  aftershocks

| Distribution<br>(parameters nu)     | Data     |            | Simulation |          |
|-------------------------------------|----------|------------|------------|----------|
|                                     | MaxLL    | BIC        | MaxLL      | BIC      |
| ML $\geq -0.2$ (29,246 Aftershocks) |          |            |            |          |
| Wald (2)                            | 97,448   | -97,431    | 97,402     | -97,393  |
| Weibull (2)                         | 100,453  | -100,444   | 99,271     | -99,263  |
| Gamma (2)                           | 98,721.9 | -98,713    | 92,588     | -92,580  |
| Loglogistic (2)                     | 101,792  | -101,784   | 92,354     | -92,346  |
| Lognormal (2)                       | 102,358  | -1,023,450 | 101,365    | -101,357 |
| Exponential (1)                     | 95,206.5 | -95,202    | 92,188     | -92,183  |
| ML $\geq 2$ (518 Aftershocks)       |          |            |            |          |
| Wald (2)                            | 15.38    | -10.97     | 12.47      | -8.06    |
| Weibull (2)                         | 100,453  | -100,444   | 99,271     | -99,263  |
| Gamma (2)                           | 98,721.9 | -98,713    | 92,588     | -92,580  |
| Loglogistic (2)                     | 101,792  | -101,784   | 92,354     | -92,346  |
| Lognormal (2)                       | 102,358  | -1,023,450 | 101,365    | -101,357 |
| Exponential (1)                     | 95,206.5 | -95,202    | 92,188     | -92,183  |

fit than the others (minimal BIC value) for the observed and synthetic aftershocks sequences. Weibull distribution is defined by

$$f(x|a, b) = ba^{-b} x^{b-1} \exp \left[ - \left( \frac{x}{a} \right)^b \right], \quad x > 0$$

The Weibull distribution parameters estimation for the interevent times of observed and synthetic aftershocks sequences are the same with regard to the confidence interval of 95%. The parameters:  $a = 0.31 \pm 0.033$ ,  $b = 0.44 \pm 0.02$ ,

i.e., the mathematical expectation is 0.8 and the variance equals 4.7.

The quality of the distribution fit can be visualized in the same way as in the case of  $ML \geq -0.2$  aftershocks. The results are shown in Figure 8. The observed and simulated curves match Weibull distribution theoretical line well. One can see some deflections of the empirical curves from the theoretical line for the interevent times fewer than 0.002 day, but a part of such data is less than 9.5%. A similar result was obtained in [Yakovlev *et al.*, 2006] for earthquake recurrence times on the San Andreas fault system. The paper provides

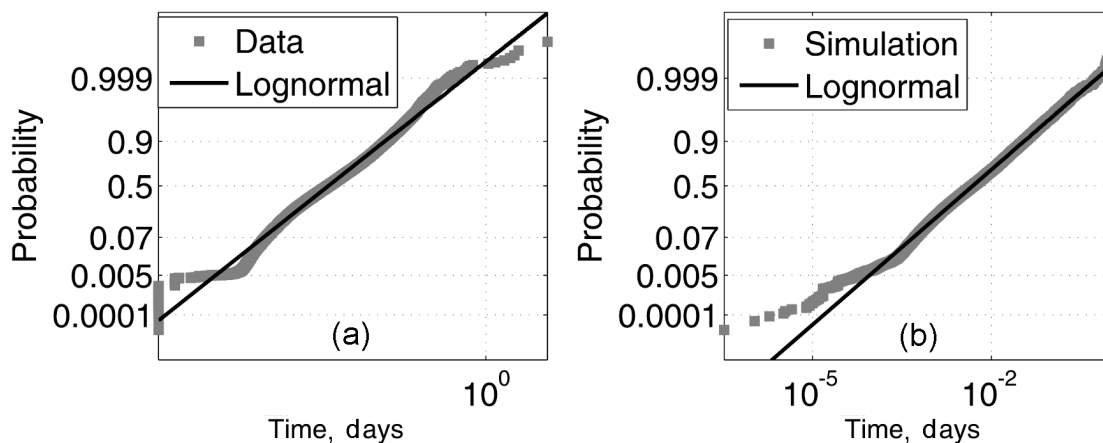


**Figure 6.** A log-log plot showing the cumulative probabilities of interevent times calculated for lognormal distribution with the estimated parameters and for the observed (a) and simulated (b) Storfjord aftershock sequences with  $ML \geq -0.2$ .

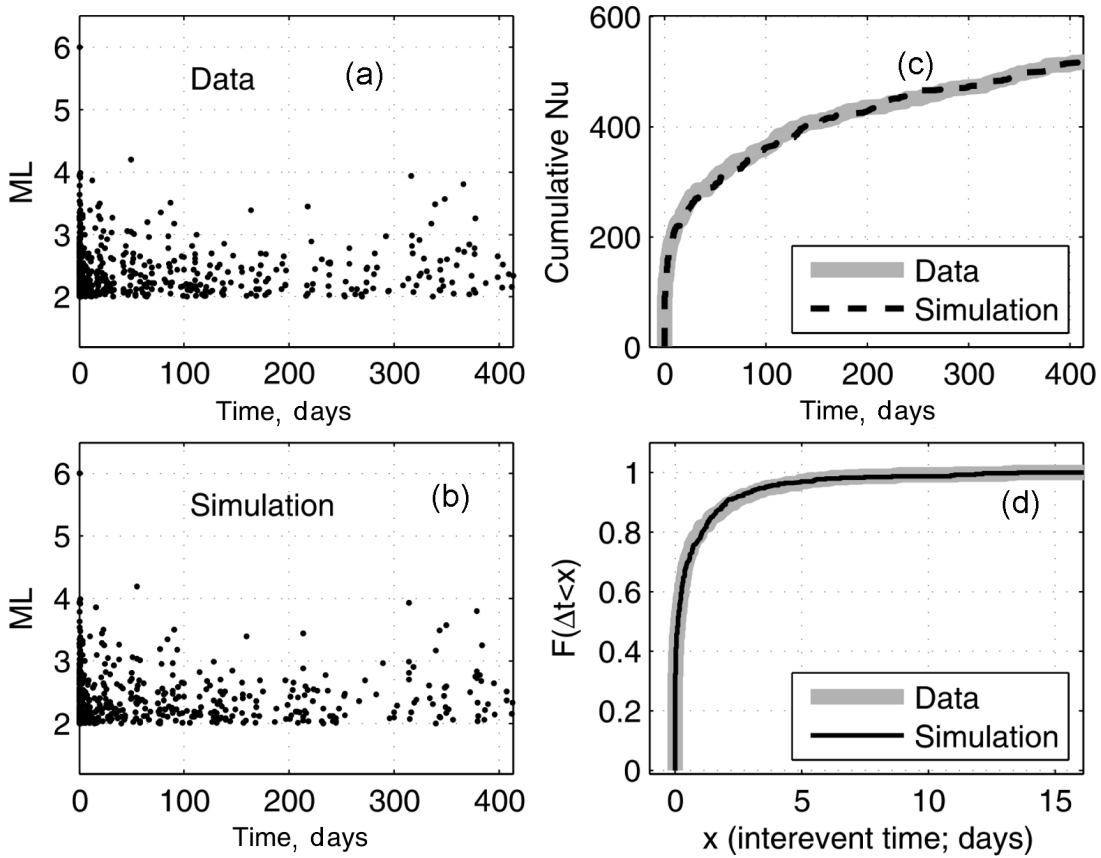


**Figure 7.** Simulation of the  $ML \geq 2$  aftershock process in Storfjord with ETAS model. (a) The observed and (b) synthetic aftershock sequences. (c) The observed and synthetic cumulative curves. (d) Empirical distribution functions of interevent times for the observed and synthetic aftershock sequences.

the expression for the hazard function in the case of Weibull distribution as well.

The ETAS model with the parameters from Table 1 accurately describes fractal interevent time statistics of the

Storfjord aftershock process with  $ML \geq 2$ . Thus, the ETAS model can be used for predicting the aftershock process and generating some seismicity scenarios by means of simulating event times.

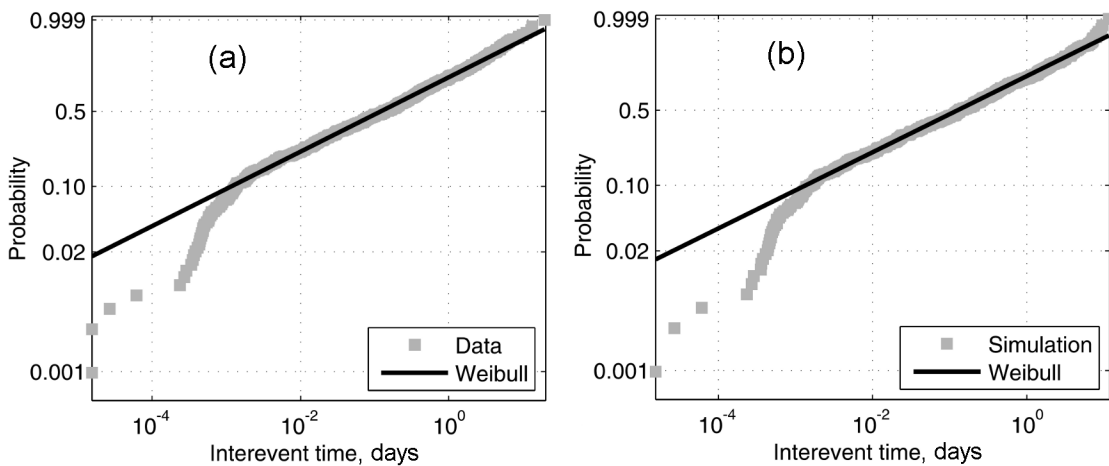


**Figure 8.** A log-log plot showing the cumulative probabilities of interevent times calculated for Weibull distribution with the estimated parameters for the observed (a) and simulated (b) Storfjord aftershock sequences with  $ML \geq 2$ .

## Discussion

The main result of the research is that the aftershock process in Storfjord is a superposition of two subprocesses, i.e. a relaxation and a trigger one. The aftershocks with  $ML \geq 2$  belong to the relaxation subprocess and the aftershocks with  $-0.2 \leq ML \leq 2$  belong to the trigger one.

Aftershock series of such a length as in Storfjord are rarely observed in intraplate conditions. As mentioned above, the best studied example is the earthquake swarms in Bohemia where a comparable number of events was observed [Fischer et al., 2005; Spichak et al., 2001; Weise et al., 2001].

It was found that movements in faults had resulted in strong shocks which destructed the drainage system of raising flows of mantle fluids in the crystal basement. So, the transportation of mantle volatiles through the crust changed the local stress field. This process caused many weak shallow earthquakes [Hainzl et al., 2005; Weise et al., 2001].

Reasoning by analogy with the Bohemian case, we suppose that the  $ML < 2$  aftershocks in Storfjord were caused by disturbance of the fluid equilibrium in the sedimentary rocks in Storfjord. This hypothesis admits the existence of a magma pocket under the aftershock area. This pocket may have caused the formation of a volcanic complex like the holocene volcano Sverre at the Northern coast of West Spitsbergen [Evdokimov, 2000]. To test this assumption one, should analyze data on the heat flow and isotope ratio of  $He^3/He^4$ . If their values are above the average meanings, it supports the assumption.

A heat flow exceeding 10 times the average meaning for the Barents Sea was revealed towards the northeast of Spitsbergen [Hutorskoy et al., 2009] at a distance of 400 km from Storfjord. The data indicate that at the depth of 4–4.5 km there are high temperatures and infiltration of the hot mantle substance into the basement and, possibly, into the low levels of the sedimentary cover. Thus, one can suggest although it is unknown whether the conditions in Storfjord are similar. Measuring of  $H^3/H^4$  ratio has not been conducted in Spitsbergen. To work out a model of Storfjord seismicity it is necessary to measure the heat flow and the  $He^3/He^4$  isotope ratio.

It is obvious that the aftershock process in Storfjord is to be comprehensively. The study will allow to verify the proposed models and obtain up-to-date information about the destruction of the continental crust at the border between the Kara Barents platform and the area of ultra slow spreading in the Norwegian, Greenlandic, and Eurasian basins.

**Acknowledgments.** The author wishes to thank Johannes Schweitzer and Myrto Pirlly (NORSAR, Norway) for their discussion which helped to improve this paper.

## References

Asming, V. E., A. V. Fedorov (2010), The improved algorithm of automatic detection and location of earthquakes by a single seismic array and its application for study of aftershock sequence in the Spitsbergen archipelago, *Seismic Instruments*, 46, 2, 48–75.

Baranov, S. V., V. E. Asming, A. N. Vinogradov (2008), Earthquake of 21.02.2008 in Storfjord, Spitsbergen, *All-Russian Conference "Northern territories of Russia: problems and develop-*

*ment perspectives"* (in Russian), Arhangelsk, 23–26 June 2008, Institute of Ecological Problems, Uro RAN, 77–80.

Benioff, H. (1962), Earthquakes and rock creep: (Part I: Creep Characteristics of Rocks and The Origin of Aftershocks), *Bulletin Bull. Seism. Soc. Am.*, 41, 1, 31–62.

Bungum, H., B. J. Mitchell, Y. Kristofferson (1982), Concentrated earthquake zones in Svalbard, *Tectonophysics*, 82, 175–188.

Crane, K., O. Eldholm, A. Myhre, E. Sundvor (1982) Thermal implications for the evolution of the Spitsbergen transform fault *Tectonophysics*, 89, 1–32.

Daley, D. J., D. A. Vere-Jones (1972), *A summary of the theory of point processes. In Stochastic Point Processes: Statistical Analysis, Theory and Applications*, Lewis P. A. W. (Ed.), N.Y., Wiley, 299–383.

Evdokimov, A. N. (2000), *Spitsbergen Volcanoes*, SPb., VNIIOkeangeologia, 123 pp.

Fischer, T., J. Horalek (2005), Slip-generated patterns of swarm microearthquakes from West Bohemia/Vogtland (central Europe): Evidence of their triggering mechanism?, *J. Geophys. Res.*, 110, B05s21, doi:10.1029/2004JB003363.

Gross, S. J., C. Kisslinger (1994), Tests of models of aftershock rate decay, *Bull. Seism. Soc. Am.*, 84, 5, 1571–1579.

Hainzl, S., Y. Ogata (2005), Detecting fluid signals in seismicity data through statistical earthquake modeling, *J. Geophys. Res.*, 110, doi:10.1029/2004JB003247.

Hutorskoy, M. D., et al. (2009), Abnormal heat flow and nature of valleys in North part of Svalbard plate, *Dokl. Akad. Nauk* (in Russian), 424, 2, 227–233.

Kisslinger, C. (1993), The Stretched Exponential Function as an Alternative Model for Aftershock Decay Rate, *J. Geophys. Res.*, 98, B2, 1913–1921.

Leonard, T., J. S. J. Hsu (1999), *Bayesian Methods, An analysis for statisticians and interdisciplinary researchers*, Cambridge Univ. Press, 335 pp.

Lewis, P. A. W., G. S. Shedler (1979), Simulation of Non-homogeneous Poisson Processes by Thinning, *Naval Res. Logistics Quart.*, 26, 403–413.

Liptzer, R. S., A. N. Shirayev (2000), *Statistics of Random Processes. II. Applications*, Springer-Verlag, New York, 402 pp.

Michael, P. J., et al. (2003), Magmatic and amagmatic seafloor generation at the ultraslow-spreading Gakkel Ridge, Arctic Ocean, *Nature*, 423, 956–961.

Narteau, C., P. Shebalin, M. Holschneider (2002), Temporal limits of the power law aftershock decay rate, *J. Geophys. Res.*, 107, B12, doi:10.1029/2002JB001868.

Ogata, Y. (1999), Seismicity Analysis through Point-process Modeling: A Review, *Pure Appl. Geophys.* 155, 471–507.

Ogata, Y., R. S. Matsu'ura, K. Katsura (1993), Fast likelihood computation of Epidemic Type Aftershock-Sequence Model, *Geophys. Res. Lett.*, 20, 19, 2143–2146.

Panasenko, G. D., E. O. Kremenetskaya, Z. I. Aranovich (1987), *Earthquake of Spitsbergen* (in Russian), Moscow, 83 pp.

Pirly, M., et al. (2010), Preliminary Analysis of the 21 February 2008, Svalbard (Norway), Seismic Sequence, *Seism. Res. Lett.*, 81, 1, 63–75.

Sholz, C. (1978), Microfractures, aftershocks, and seismicity, *Bull. Seismol. Soc. Am.*, 58, 1117–1130.

Spichak, A., J. Horalek (2001), Possible role of fluids in the process of earthquake swarm generation in West Bohemia/Vogtland seismoactive region, *Tectonophysics*, 336, 151–161.

Utsu, T. A. (1961), A statistical study on the occurrence of aftershocks, *Geoph. Magazine*, 30, 521–605.

Weise, S. M., et al. (2001), Transport of mantle volatiles through the crust traced by seismically release fluids: a natural experiment in the earthquake swarm area Vogland/NW Bohemia, Central Europe, *Tectonophysics*, 336, 137–150.

Yakovlev, G., D. L. Turcotte, J. B. Rundle J. B., P. B. Rundle (2006), Simulation-Based Distributions of Earthquake Recurrence Times on the San Andreas Fault System, *Bull. Seism. Soc. Am.*, 96, 6, 1995–2007.

S. V. Baranov, Kola Branch of Geophysical Survey of RAS, 14 Fersmana st., 184209 Apatity, Russia. (bars.vl@gmail.com)